VARIATION OF INTRACELLULAR CA^{2+} FOLLOWING CA^{2+} CURRENT IN HEART

A Theoretical Study of Ionic Diffusion Inside a Cylindrical Cell

RODOLPHE FISCHMEISTER AND MAGDA HORACKOVA
Department of Physiology and Biophysics, Faculty of Medicine, Dalhousie University, Halifax, Nova Scotia, Canada B3H 4H7

ABSTRACT The variation in the concentration of a diffusing substance inside a cylindrical cell submitted to a time-dependent flux at the sarcolemmal membrane was studied theoretically. An application was derived to estimate the local modifications of intracellular free Ca^{2+} concentration ($[Ca^{2+}]_i$) induced by the slow inward Ca^{2+} current (I_{Ca}) in frog heart. During a 0 mV voltage clamp depolarization, $[Ca^{2+}]_i$ at the inner side of the membrane rises earlier and faster than $[Ca^{2+}]_i$ at the center of the cell. The binding of intracellular Ca^{2+} to specific sites enhances the deviation between the two concentrations and may generate an accumulation-depletion process of Ca^{2+} near the membrane. However, it also decreases the overall $[Ca^{2+}]_i$. The relatively slow diffusion of sarcoplasmic Ca^{2+} does not significantly affect the kinetics of I_{Ca} through a modification in the Ca^{2+} gradient across the membrane.

INTRODUCTION

The variations of the intracellular Ca^{2+} concentration ($[Ca^{2+}]_i$) in excitable cells are of general interest because Ca^{2+} plays a critical role in excitation-contraction coupling in muscle, in the release of synaptic transmitters from nerve terminals, and in the control of various membrane permeabilities. For those effects that take place at the sarcolemmal membrane (such as the activation by Ca^{2+} of a K^+ channel [Meech, 1972; Isenberg, 1977], the activation of a nonspecific inward channel [Colquhoun et al., 1981], and the inactivation of the Ca^{2+} channel [Tillotson, 1979; D. Mentrard, G. Vassort, and R. Fischmeister, manuscript submitted for publication]), the determinant factor is the $[Ca^{2+}]$ at the inner side of the membrane. This may substantially differ from the $[Ca^{2+}]$ deeper in the cell (Gorman and Thomas, 1980; Levy et al., 1982), and the gradient of $[Ca^{2+}]$ at the membrane may be subject to larger variations than the overall $[Ca^{2+}]_i$ (Bassingthwaighte and Reuter, 1972). This noninstantaneous diffusion of Ca^{2+} may affect the transmembrane transport of Ca^{2+} itself. In particular, the decrease of the Ca^{2+} gradient may participate in, or be responsible for, the apparent inactivation of the Ca^{2+} current together with, or rather than, a direct effect of Ca^{2+} ions on specific sites controlling the Ca^{2+} conductance (Tillotson, 1979; Eckert and Tillotson, 1981; D. Mentrard, G. Vassort, and R. Fischmeister, manuscript submitted for publication).

The diffusion of Ca^{2+} in the sarcoplasm is slower than would be expected from its free diffusion coefficient in water (Niedergerke, 1957; Blaustein and Hodgkin, 1969; Kushmerick and Podolsky, 1969; Bassingthwaighte and Reuter, 1972; Gorman and Thomas, 1980). This slowing down of Ca^{2+} diffusion has been attributed mainly to the binding of Ca^{2+} to specific sites and buffering systems (e.g., contractile proteins, sarcoplasmic reticulum, mitochondria). The way binding reactions modify the diffusional process has been theoretically studied by Crank (1975) in a plane, a cylinder, and a sphere, and has been applied to various experimental conditions (Roughton, 1959; Vieth and Sladek, 1965; Blaustein and Hodgkin, 1969; Safford and Bassingthwaighte, 1977; Gorman and Thomas, 1980). However, in all these works, the diffusional process was assumed to result from a transfer of diffusing substance at a constant rate, during a transient or long period. In contrast, the transfer of ions across the sarcolemmal membrane of excitable cells occurs normally through gated and nongated ionic channels; the currents generated show a complex time dependence. Thus, unless severe approximations are made, the existing models cannot be used properly to estimate local modifications of intracellular ionic concentrations such as those following a voltage-clamp depolarization.

The present study gives a theoretical analysis of the variation in the concentration of a diffusing substance inside a cylindrical cell submitted to a time-dependent flux

Dr. Fischmeister was a postdoctoral fellow of the Nova Scotia Heart Foundation. His permanent address is Laboratoire de Physiologie Cellulaire Cardiaque, Bât. 443, Université de Paris Sud, F-91405, Orsay, France.

at the surface when (*a*) the diffusion coefficient is constant (no binding reaction) or (*b*) the diffusion is modified by binding reactions leading to an apparent diffusion coefficient, which is a function of the concentration itself. The equations are then applied to results obtained from frog cardiac cells for the study of the slow inward Ca^{2+} current, I_{Ca} or I_{si}, generated by a voltage-clamp depolarization, and the corresponding variations of $[Ca^{2+}]_i$. The possible participation of sarcoplasmic Ca^{2+} accumulation to the inactivation of I_{Ca} through a reduction in the driving force for Ca^{2+} is examined.

GLOSSARY

t	time (seconds).
a	cell radius (centimeters).
r	radial coordinate, $0 \le r \le a$ (centimeters).
$C(r, t)$	concentration of the diffusing substance C (molars).
C_0	concentration of C at $t = 0$ and $0 \le r \le a$ (molars).
D	diffusion coefficient of C when there are no binding sites for C or all binding sites are at saturation ($cm^2 \cdot s^{-1}$).
$\phi(t)$	rate of transfer of C per unit area of the membrane ($mol \cdot cm^{-2} \cdot s^{-1}$).
$I(t)$	transarcolemmal ionic current ($A \cdot cm^{-2}$).
i, j, n	indices.

Model I

$\bar{C}(r, p), \bar{\phi}(p)$	Laplace transforms of C and ϕ.
q^2	$= p/D$.
I_0, I_1	modified Bessel functions of order 0 and 1.
J_0, J_1	ordinary Bessel functions of order 0 and 1.
α_n	nth positive root of $J_1(\alpha) = 0$.
β_n	nth positive root of $\beta\cot(\beta) = 1$.
Δt	interval for time integration (seconds).
$C_i(r), \phi_i$	values of C and ϕ at $t_i = i\,\Delta t$.

Model II

B_{Ti}, B_i	total and free concentration of binding sites B_i (molars).
K_{bi}	affinity constant of B_i for C (M^{-1}).
N_b	number of different binding sites B_i ($i = 1 \rightarrow N_b$).
D_{app}	apparent diffusion coefficient of unbound C ($cm^2 \cdot s^{-1}$).
R	$= r/a$.
θ	$= Dt/a^2$.
$\Delta R, \Delta\theta$	intervals for radial and time integrations.
R_j	$= j \cdot \Delta R$ ($j = 0 \rightarrow N$; $N \cdot \Delta R = 1$).
θ_n	$= n \cdot \Delta\theta$.
$C_{j,n}$	$= C(R_j, \theta_n)$.

METHODS

The cell is considered to be a long, circular cylinder in which diffusion is radial everywhere. If a is the radius (centimeters) and D the diffusion coefficient ($cm^2 \cdot s^{-1}$), the concentration, C (molars), of the diffusing substance is a function solely of radial distance, r (centimeters), and time, t (seconds). The diffusion equation (Crank, 1975) is

$$\frac{\partial C}{\partial t} = \frac{1}{r}\frac{\partial}{\partial r}\left(rD\frac{\partial C}{\partial r}\right) \quad 0 \le r < a; \quad t > 0. \tag{1}$$

The boundary conditions can be expressed as

$$C(r, t) = C_0 \quad 0 \le r \le a; \quad t = 0 \tag{2}$$

assuming that the initial concentration C_0 (molars) is constant, i.e., the cell is in a steady-state before stimulation, and

$$-D\frac{\partial C}{\partial r} = \phi \quad r = a; \quad t > 0, \tag{3}$$

where $\phi(t)$ is the rate of transfer of diffusing substance per unit area of the membrane ($mol \cdot cm^{-2} \cdot s^{-1}$). If C is the concentration of an ion that crosses the sarcolemmal membrane by generating a single ionic current I ($A \cdot cm^{-2}$), then

$$\phi = \frac{1}{zF} I, \tag{4}$$

where z is the valence and F the Faraday constant.

Model I: Resolution of Eqs. 1–3 When the Diffusion Coefficient D is Constant

By using the Laplace transformation, Eq. 1 becomes (Carslaw and Jaeger, 1959, p. 327)

$$\frac{\partial^2 \bar{C}}{\partial r^2} + \frac{1}{r}\frac{\partial \bar{C}}{\partial r} - q^2\bar{C} = 0 \quad 0 \le r < a, \tag{5}$$

where $\bar{C}(r, p)$ is the Laplace transform of $C(r, t)$, and $q^2 = p/D$. The boundary condition, Eq. 3, can be written

$$\frac{\partial \bar{C}}{\partial r} = -\frac{\bar{\phi}}{D} \quad r = a, \tag{6}$$

where $\bar{\phi}(p)$ is the Laplace transform of $\phi(t)$. The solution of Eqs. 5 and 6 is

$$\bar{C} = -\frac{\bar{\phi}}{p^{1/2}D^{1/2}}\frac{I_0(qr)}{I_1(qa)}. \tag{7}$$

I_0 and I_1 are the modified Bessel functions of order 0 and 1, respectively. Eq. 7 can be written

$$\bar{C} = \bar{\phi} \cdot \bar{b}, \tag{8}$$

where $\bar{b}(p, r)$ is the Laplace transform of a function $b(t, r)$. b is then given by the inversion theorem:

$$b = \frac{1}{2\pi i D^{1/2}} \int_{\gamma - i\infty}^{\gamma + i\infty} e^{\lambda t}\frac{I_0(\mu r)}{\lambda^{1/2} I_1(\mu a)}\,d\lambda, \tag{9}$$

where μ is written for $(\lambda/D)^{1/2}$. The integral of Eq. 9, evaluated with the residue theorem, yields

$$b = \frac{2}{a} + \frac{2}{a}\sum_{n=1}^{\infty} \exp(-D\alpha_n^2 t/a^2)\frac{J_0(r\alpha_n/a)}{J_0(\alpha_n)}, \tag{10}$$

where α_n is the nth positive root of

$$J_1(\alpha) = 0. \tag{11}$$

J_0 and J_1 are the Bessel functions of order 0 and 1, respectively. The inversion theorem applied to Eq. 8 gives C as a convolution function of b and ϕ; with Eq. 2 our final solution is

$$C = C_0 - \frac{2}{a}\int_0^t \phi(\tau) \cdot d\tau - \frac{2}{a}\sum_{n=1}^{\infty} \exp(-D\alpha_n^2 t/a^2) \cdot \frac{J_0(r\alpha_n/a)}{J_0(\alpha_n)} \int_0^t \exp(D\alpha_n^2\tau/a^2) \cdot \phi(\tau)\,d\tau. \tag{12}$$

If ϕ is a constant, time-independent function, then Eq. 12 becomes the solution given by Crank (1975) for a constant flux at the surface.

If ϕ is not an analytical function, the integrals of Eq. 12 have to be evaluated numerically. With Δt being the interval for time integration, and C_i and ϕ_i the values of C and ϕ at $t_i = i \cdot \Delta t$, then

$$C_i = C_0 - \frac{2}{a} \cdot \Delta t \left[\sum_{j=0}^{i} \phi_j + \sum_{n=1}^{\infty} \exp(-D\alpha_n^2 i \Delta t / a^2) \cdot \frac{J_0(r\alpha_n/a)}{J_0(\alpha_n)} \sum_{j=0}^{i} \exp(D\alpha_n^2 j \Delta t / a^2) \phi_j \right], \quad (13)$$

which gives the concentration at any radial distance $0 \le r \le a$.

In the case of a spherical cell of radius a, a similar demonstration gives the solution

$$C = C_0 - \frac{3}{a} \int_0^t \phi(\tau) \cdot d\tau - \frac{2}{a} \sum_{n=1}^{\infty} \frac{\sin(\beta_n r/a)}{\sin(\beta_n)} \cdot \exp(-D\beta_n^2 t/a^2) \int_0^t \exp(D\beta_n^2 \tau / a^2) \phi(\tau) \cdot d\tau, \quad (14)$$

where β_n is the nth positive root of

$$\beta \cdot \cot(\beta) = 1. \quad (15)$$

Model II: Resolution of Eqs. 1–3 When the Diffusion is Modified Due to Binding Reactions

In this section, we follow the assumptions and the proposal made by Bassingthwaighte and Reuter (1972) and Safford and Bassingthwaighte (1977). Namely, (*a*) the rate of change of concentration C of the diffusing substance C at a point is influenced by first-order bindings to immobile substances B_i, forming complexes CB_i, and (*b*) the rate constants of binding and release are very fast compared to mass-transport rates across the membrane, so that the bindings are always essentially at equilibrium. Then, the apparent diffusion coefficient, D_{app}, of unbound substance C is a function of the concentration (Safford and Bassingthwaighte, 1977)

$$D_{app} = \frac{D}{1 + \sum_{i=1}^{N_b} K_{bi} \cdot B_{Ti} / (1 + K_{bi} \cdot C)^2}, \quad (16)$$

where N_b is the number of different immobile binding sites for C; B_{Ti} is the total concentration of binding site B_i (molars); $K_{bi} = CB_i / C \cdot B_i$ is the affinity constant of the binding site $B_i (M^{-1})$; and D is now the diffusion coefficient of C when all the binding sites are saturated. For convenience, Eq. 16 can be written

$$D_{app} = \frac{D}{h(C)}. \quad (17)$$

The appropriate diffusion equation is now

$$\frac{\partial}{\partial R}\left(R \frac{\partial C}{\partial R}\right) = R \cdot h(C) \cdot \frac{\partial C}{\partial \theta} \qquad 0 \le R < 1; \quad \theta > 0 \quad (18)$$

with the substitutions $R = r/a$ and, $\theta = (D \cdot t)/a^2$. The boundary condition (Eq. 3) becomes

$$-\frac{D}{a} \frac{\partial C}{\partial R} = \phi \qquad R = 1; \quad \theta > 0. \quad (19)$$

A diffusion equation similar to Eq. 18, but applied to a plane, was obtained by Vieth and Sladek (1965) for the diffusion in glassy polymer. As they did, we used the finite-difference method described by Douglas (1958) to approximate Eq. 18 numerically. Let $C_{j,n} = C(R_j, \theta_n)$, with $R_j = j \cdot \Delta R$ ($j = 0, N$; $N \cdot \Delta R = 1$) and $\theta_n = n \cdot \Delta\theta$; two equations are used to proceed from values of $C_{j,n}$ to values at the next time step $C_{j,n+1}$

$$\Delta_R(R_j \Delta_R C_{j,n}) = R_j \cdot h(C_{j,n}) \cdot (C_{j,n+1/2} - C_{j,n}) \cdot \frac{2}{\Delta\theta}, \quad (20)$$

$$\frac{1}{2}\left[\Delta_R(R_j \cdot \Delta_R C_{j,n+1}) + \Delta_R(R_j \cdot \Delta_R C_{j,n})\right] = R_j \cdot h(C_{j,n+1/2}) \cdot (C_{j,n+1} - C_{j,n}) \frac{1}{\Delta\theta} \quad (21)$$

with the second-order finite difference $\Delta_R(R_j \cdot \Delta_R C_{j,n})$ given by

$$\Delta_R(R_j \cdot \Delta_R C_{j,n}) = \frac{[(j+1/2) \cdot (C_{j+1,n} - C_{j,n})] - [(j-1/2) \cdot (C_{j,n} - C_{j-1,n})]}{\Delta R}. \quad (22)$$

Eq. 21 gives an estimate of Eq. 18, which is time-centered around $(n + 1/2)\Delta\theta$. This leads to a set of linear, algebraic equations, provided that $h(C_{j,n+1/2})$ is known. This is achieved by the forward-difference estimate of $C_{j,n+1/2}$ given by Eq. 20. A relatively simple algorithm is then used to derive the solution of Eq. 21 with the boundary conditions (Eqs. 2 and 19), and the integration can proceed.

Application to the Variations of Intracellular Ca^{2+} Concentration Induced by the Slow Inward Ca^{2+} Current in Frog Cardiac Cells

The two models have been applied in frog heart to the transsarcolemmal movement of Ca^{2+} induced by the slow inward Ca^{2+} current I_{Ca}($\mu A \cdot cm^{-2}$) and the resulting variations of sarcoplasmic Ca^{2+} concentration $[Ca^{2+}]_i$. The equations were programmed in FORTRAN IV and solved on a Sigma 5 computer (Xerox Corp., Stamford, CT).

Particular attention was devoted to the accuracy of the numerical integration. For the first model, a value of Δt was considered as acceptable for a given integration when the same integration performed with $\Delta t/2$ gave a maximal relative difference of 1%. In the numerical applications considered, the size of Δt varied from 0.01 to 0.1 ms. To perform an accurate solution with the second model required an adequate choice of both $\Delta\theta$ and ΔR. In the special case $h(C) = 1$ and $D_{app} = D$ (i.e., no binding reaction), the solutions obtained with the two models are theoretically identical. Values of $\Delta\theta$ and ΔR were considered acceptable when the two integrated solutions differed by <0.2%. Generally, ΔR equaled $1/200$ and $\Delta\theta$ varied from 5×10^{-4} to 5×10^{-3}. The total computation time could vary from 5 to 25 min for a 200-ms interval of integration.

The classical Hodgkin-Huxley, purely voltage-dependent interpretation of I_{Ca} kinetics has been found to be not fully satisfactory in frog heart (Fischmeister et al., 1981; Fischmeister and Horackova, 1982; D. Mentard, G. Vassort, and R. Fischmeister, manuscript submitted for publication). This model does, however, give a relatively good approximation of the voltage-clamp data obtained for 0 to 10-mV membrane depolarizations. Therefore, I_{Ca} was described as

$$I_{Ca} = \bar{g}_{Ca} \cdot d \cdot f \cdot (E_m - E_{Ca}), \quad (23)$$

where $\bar{g}_{Ca}$ is the maximal Ca^{2+} conductance ($mS \cdot cm^{-2}$); d and f are the activation and inactivation gating variables, respectively; and E_m and E_{Ca} are the membrane and I_{Ca}-reversal potentials (millivolts), respectively.

The gating variables satisfy the first-order differential equation

$$\frac{dy}{dt} = \alpha_y \cdot (1 - y) - \beta_y \cdot y, \quad (24)$$

where $y = d$ or f and the rate constants α_y and β_y (ms^{-1}) are specifically voltage-dependent. Their variations are given by

$$\alpha_d = \frac{0.1 \exp [0.103(E_m + 16.7)]}{1 + \exp [0.088(E_m + 16.7)]} \quad (25)$$

$$\beta_d = \frac{0.078 \exp [-0.089(E_m + 25.2)]}{1 + \exp [-0.065(E_m + 25.2)]} \quad (26)$$

$$\alpha_f = \frac{0.0085 \exp [-0.311(E_m + 21.8)]}{1 + \exp [-0.256(E_m + 21.8)]} \quad (27)$$

$$\beta_f = \frac{0.01 \exp [0.201(E_m + 36.8)]}{1 + \exp [0.172(E_m + 36.8)]}. \quad (28)$$

Eqs. 25 and 26 were used in a previous study to describe the activation of Ca current in frog heart (Fischmeister and Horackova, 1982). Eqs. 27 and 28 were calculated from the original experimental data of Horackova and Vassort (1976). In the following simulations, I_{Ca} is calculated with a maximal conductance $g_{Ca} = 0.11$ mS · cm^{-2}. E_{Ca} is described as the Nernst equilibrium potential for Ca^{2+} at 20°C

$$E_{Ca} = 12.6 \log \frac{[Ca^{2+}]_o}{[Ca^{2+}]_i(a)}, \quad (29)$$

where the extracellular concentration $[Ca^{2+}]_o$ is set at 1.8 mM, and $[Ca^{2+}]_i(a)$ is the intracellular concentration at the inner side of the membrane ($r = a$). In the initial conditions, at rest, $[Ca]_i$ is assumed to be independent of r and is set at $C_0 = 10^{-7}$ M ($0 \le r \le a$).

Note that, because $[Ca^{2+}]_i(a)$ is directly dependent on the diffusional process of intracellular Ca^{2+}, modifications of this process will induce variations in I_{Ca} through changes in E_{Ca}. However, the numerical values given above for the activation, inactivation, and maximal conductance of the Ca^{2+} channel were chosen so that our simulated I_{Ca} would resemble in amplitude and time course those recorded in frog atrial preparations during a 0-mV voltage-clamp step (e.g., Horackova and Vassort, 1979).

The radius a of the cylindrical cell is calculated as $2/(S/V)$, where S/V is a cell's surface/volume ratio (cm^{-1}). Morphological studies of frog cardiac cells by Page and Niedergerke (1972) and Hoerter et al. (1981) give $S/V \sim 13{,}000$ cm^{-1}, which leads to the value $a \sim 1.5$ μm taken in our computations. This value agrees well with mean diameters we obtained from measuring 20 single, enzymatically isolated cells of *Rana pipiens* and of *Rana catesbiana*, 3.9 and 6.8 μm, respectively (M. Horackova, unpublished results). Hume and Giles (1981) have reported 4–7 μm for bullfrog atrial cells.

The free-diffusion coefficient for calcium in aqueous solution, D^0_{Ca}, is 7.78×10^{-6} cm^2/s (Wang, 1953). However, much smaller values have been reported for the diffusion coefficient for calcium in muscle, D_{Ca}: $D_{Ca} = D^0_{Ca}/16$ in frog heart (Niedergerke, 1957); $D_{Ca} = D^0_{Ca}/50$ in frog skeletal muscle (Kushmerick and Podolsky, 1969); $D_{Ca} = 0.21\ D^0_{Ca}$ in mammalian heart, at steady-state (Safford and Bassingthwaighte, 1977). To account for this variability in the experimental results, our simulations were performed with different values of D_{Ca}.

RESULTS

Substituting $[Ca^{2+}]_i$, D_{Ca}, and I_{Ca} for C, D, and I, respectively, in Eqs. 1–4 and elsewhere, and with the numerical values given in the Methods section, numerical solutions for $[Ca^{2+}]_i$ can be derived from the two models described above, provided that D_{Ca} (for the two models), and N_b, K_{bi}, and B_{Ti} (Eq. 16; for the second model only) are known. Solutions are computed during single 200-ms voltage-clamp steps at $E_m = 0$ mV, from a holding potential equal to the resting potential, $E_r = -85$ mV. $[Ca^{2+}]_i$ could be calculated at any distance $r (0 \le r \le a)$ from the longitudinal axis of the cylindrical cell. However, for the sake of simplicity and clarity, only $[Ca^{2+}]_i(0)$ and $[Ca^{2+}]_i(a)$ are given here, which correspond to the two extreme positions $r = 0$ (i.e., on the longitudinal axis) and $r = a$ (i.e., at the inner side of the sarcolemmal membrane), respectively.

Fig. 1 shows simulations using the first model, i.e., assuming that all Ca^{2+} entering the cell through the calcium channel remains free inside the cell and D_{Ca} is constant. This might either mean that there is no binding site for intracellular Ca^{2+} or that the binding sites are already saturated at the low initial free Ca^{2+} concentration C_0. Certainly, neither of these assumptions is applicable to Ca^{2+} in muscle (although they might be applicable to other ions, such as Na^+ and K^+). However, these simulations give an upper limit for the variations of $[Ca^{2+}]_i$ induced by I_{Ca} and allow us to evaluate the effect of the diffusional process.

The curves of $[Ca^{2+}]_i(a)$ (Fig. 1 *a*) and $[Ca^{2+}]_i(0)$ (Fig. 1 *b*) show that, except during the first 5 ms, when $D_{Ca} = D^0_{Ca}$ (curves 1), the time course of $[Ca^{2+}]_i$ at the center of the cell closely follows that at the sarcolemmal membrane. Moreover, these two curves are similar to the variation of $[Ca^{2+}]_i$ (not shown) obtained when the diffusion of Ca^{2+} inside the cell is assumed to be instantaneous. Variations of $[Ca^{2+}]_i(a)$ and $[Ca^{2+}]_i(0)$ start to differ significantly when $D_{Ca} = D^0_{Ca}/15$ (curves 3). When the diffusion coefficient is further decreased (curves 4–8), $[Ca^{2+}]_i$ at the membrane increases faster (Fig. 1 *a*), whereas the rise in the concentration at the center becomes slower (Fig. 1 *b*) and occurs after a longer delay (up to 50 ms when $D_{Ca} = D^0_{Ca}/300$; Fig. 1 *b*, curve 8). Simultaneously, an accumulation-depletion of Ca^{2+} occurs at the inner side of the membrane when $D_{Ca} < D^0_{Ca}/100$ (Fig. 1 *a*, curves 6–8).

The influence of the diffusional process of sarcoplasmic Ca^{2+} on I_{Ca} is shown in Fig. 1 *d*. When D_{Ca} is decreased (curves 1–8), the peak amplitude of I_{Ca} is decreased (by ~20% in curve 8, when $D_{Ca} = D^0_{Ca}/300$), whereas the apparent time constants of activation and inactivation are unaffected or only slightly increased. These modifications of I_{Ca} are due to the changes in the time course of E_{Ca} (Fig. 1 *c*). The small effects observed on the kinetics of I_{Ca}, in particular on its inactivation, rule out the possibility of a significant participation of the reduction in E_{Ca} to the inactivation of I_{Ca} (see Discussion).

Fig. 2 shows simulated variations of $[Ca^{2+}]_i$ (Fig. 2 *a–c*) and I_{Ca} (Fig. 2 *d*) obtained with the second model, i.e., assuming that the diffusion of Ca^{2+} in the sarcoplasm is affected by first-order binding reactions. No Ca^{2+}-dependent release of Ca^{2+} from internal stores was considered to modify $[Ca^{2+}]_i$ in our simulations; this is consistent with the indication that these stores are not markedly present in

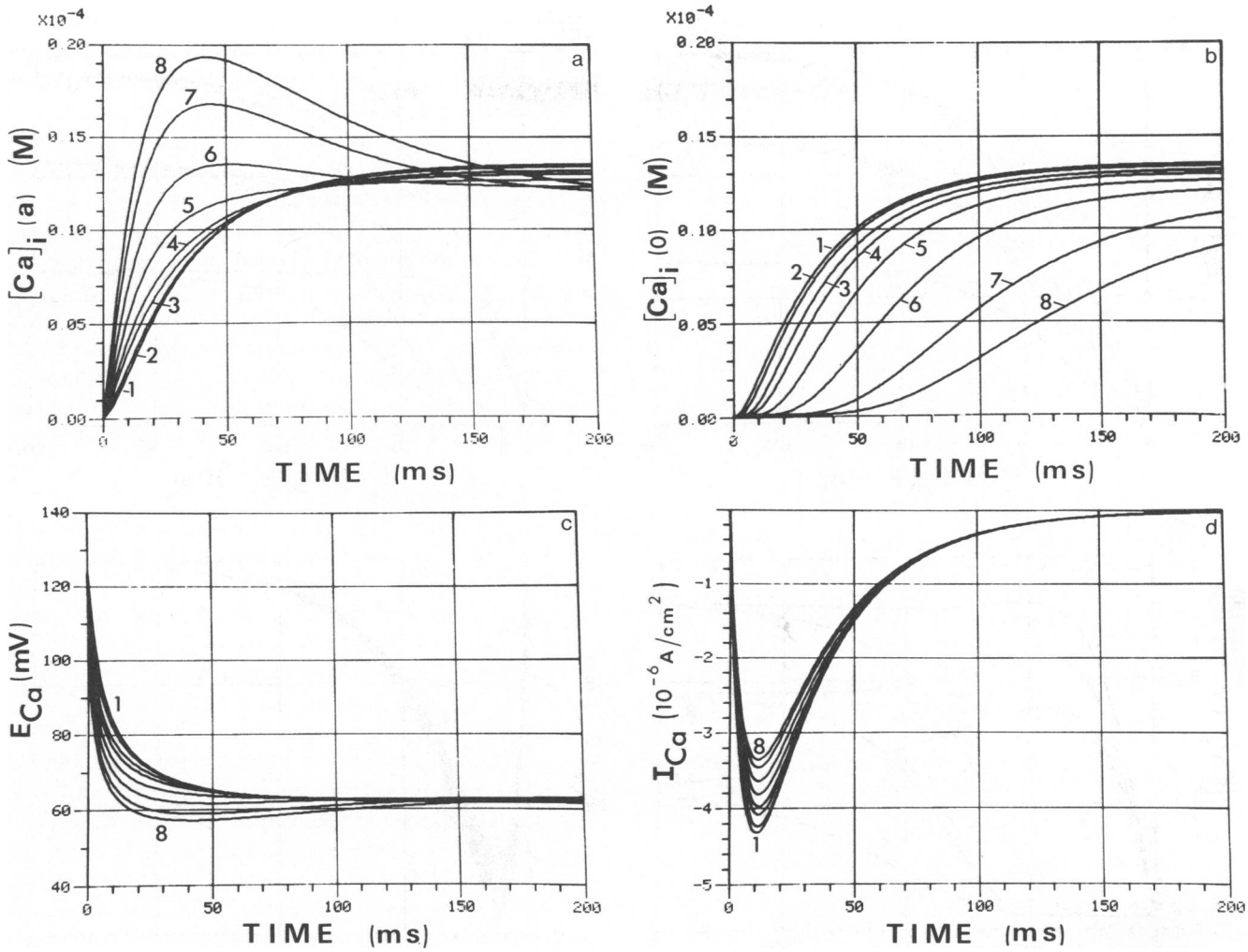

FIGURE 1 Simulations of Ca^{2+} parameters during a 0-mV, 200-ms voltage-clamp depolarization (from $E_r = -85$ mV), using a model of constant diffusion coefficient, D_{Ca}. D_{Ca} is given relatively to the diffusion coefficient of calcium in water, $D^0_{Ca} = 7.78 \times 10^{-6}$ cm^2 · s^{-1}. D^0_{Ca}/D_{Ca} is 1, 5, 15, 25, 50, 100, 200, and 300 respectively, for curves 1–8. (*a*) $[Ca^{2+}]_i(a)$, intracellular calcium concentration at the inner side of the sarcolemmal membrane; (*b*) $[Ca]_i(0)$, intracellular calcium concentration at the center of the cell; (*c*) E_{Ca}, reversal potential of Ca^{2+} current I_{Ca}; (*d*) I_{Ca}.

frog heart (Fabiato and Fabiato, 1978). For the sake of simplicity, we assumed, as did Bassingthwaighte and Reuter (1972), that troponin is the main binding site for Ca^{2+}, i.e., $N_b = 1$ in Eq. 16. Katz (1970) estimated to $\sim 6.7 \times 10^{-5}$ M the total concentration of troponin in cardiac cells, with an affinity to Ca^{2+} of 3.4×10^5 to 1.5×10^6 M^{-1}. Allen and Blinks (1978) reported a value of $\sim 2 \times 10^{-6}$ M in frog heart for the free $[Ca^{2+}]_i$ accompanying a twitch. Using this order of magnitude, we investigated in our calculations two different concentrations of binding sites for Ca^{2+} (B_T in Eq. 16), 2.6×10^{-5} and 5×10^{-5} M, and two different affinities (K_b in Eq. 16), 5×10^5 and 10^6 M^{-1}.

As with the first model, decreasing D_{Ca} accentuates the deviation between $[Ca^{2+}]_i(a)$ and $[Ca^{2+}]_i(0)$ and develops an increasing delay during which $[Ca^{2+}]_i(0)$ is not significantly affected by the influx of Ca^{2+} at the surface. These two effects are considerably enhanced when either B_T or K_b is increased. This is explained by the decrease of D_{app} (Eq. 16). A phenomenon of accumulation-depletion of Ca^{2+} may occur at the membrane when D_{app} is further decreased (curves 7 and 8, Fig. 2 *c*). However, increasing B_T and K_b not only decreases the D_{app} of free Ca^{2+}, but also reduces the overall free $[Ca^{2+}]_i$. Although the modifications in $[Ca^{2+}]_i(a)$ induced by different situations examined are relatively large, the corresponding variations of I_{Ca} are small (Fig. 2 *d*). The peak value is increased by increases in B_T and/or K_b for a given D_{Ca} (although D_{app} is smaller), but decreasing D_{Ca} alone reduces the maximal amplitude of I_{Ca} (as also shown in Fig. 1 *d*). The kinetics of I_{Ca} are not significantly affected by the diffusional process of intracellular Ca^{2+}.

DISCUSSION

In excitable cells different ions, mainly Na^+, K^+, and Ca^{2+}, cross the sarcolemma through specific ionic channels,

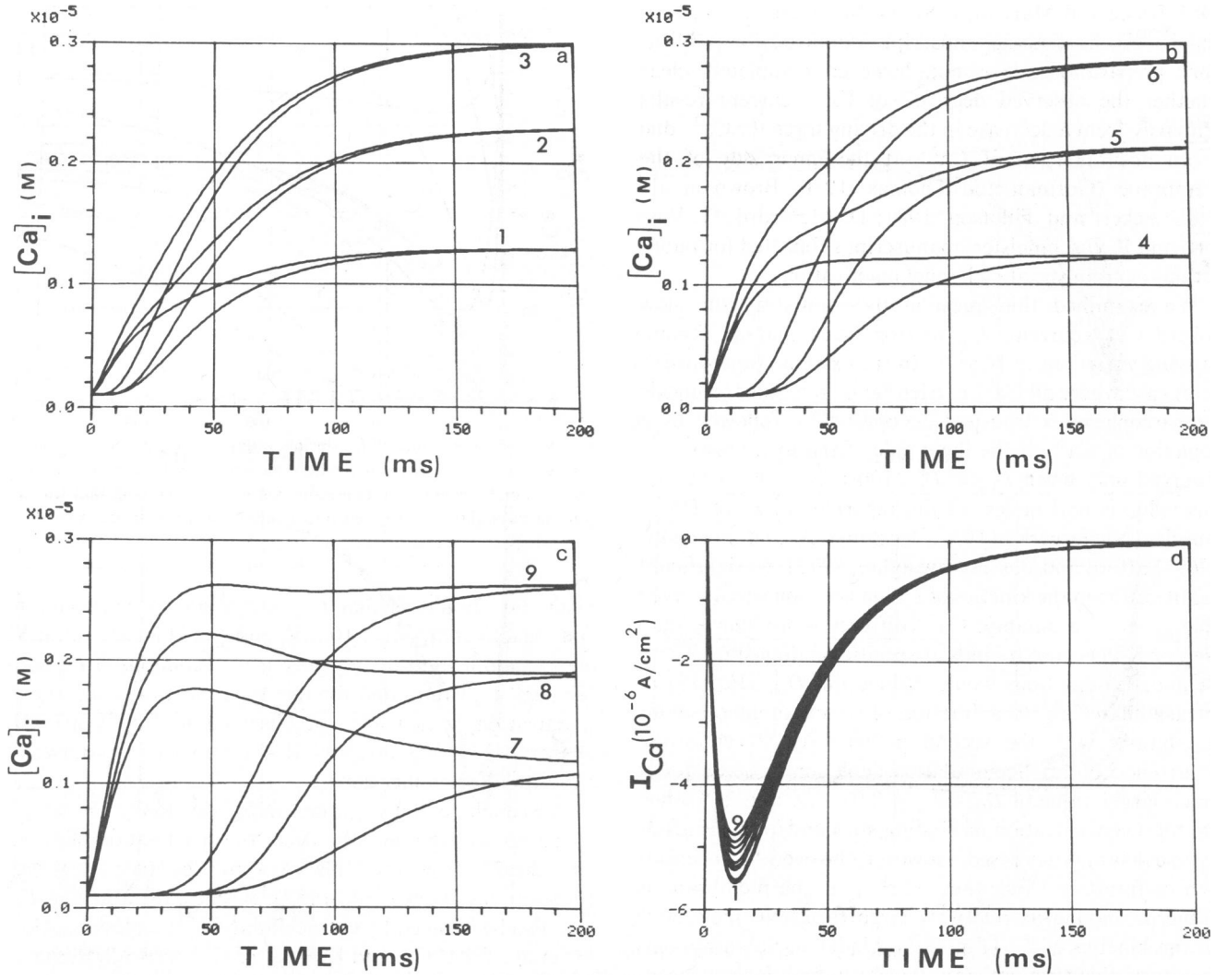

FIGURE 2 Simulations of calcium parameters during a 0-mV, 200-ms voltage-clamp depolarization (from $E_r = -85$ mV), using a model of diffusion with binding reactions. (*a–c*) Intracellular calcium concentration: each set of two curves (1–9) gives $[Ca^{2+}]_i(a)$ on the upper curve and $[Ca^{2+}]_i(0)$ on the lower. D_{Ca}/D^0_{Ca} is 0.63 in *a*, 0.21 in *b*, and 0.07 in *c*. The concentration of binding sites, B_T, and the affinity of these sites for calcium, K_b, are, respectively, 2.6×10^{-5} M and 5×10^5 M^{-1} for curves 3, 6, and 9; 2.6×10^{-5} M and 10^6 M^{-1} for curves 2, 5, and 8; 5×10^{-5} M and 5×10^5 M^{-1} for curves 1, 4, and 7. (*d*) I_{Ca}.

generating transmembrane ionic currents. These currents, which are voltage- and time-dependent, may also be affected by the concentrations of the respective ions near the membrane. The two models developed in this study allow us to estimate the contribution of the diffusional process to the distribution, inside the sarcoplasm, of ions crossing the sarcolemmal membrane of a cylindrical or spherical cell.

The diffusion of Na^+ and K^+ in the sarcoplasm is similar to that in water, in nerve (Palti et al., 1979), or two times slower in muscle (Kushmerick and Podolsky, 1969), showing that chemical interactions do not limit the mobility of these ions. The constant diffusion-coefficient model (Model I) can be used to derive the modifications of $[Na^+]_i$ and $[K^+]_i$ following the fast inward Na^+ current and the outward K^+ currents in nerve or heart, during an action potential or under voltage-clamp conditions.

In this study, we have calculated how $[Ca^{2+}]_i$ would vary with transmembrane Ca^{2+} current. Besides regulating excitation-contraction coupling in muscle and releasing synaptic transmitters from nerve terminals, Ca^{2+} controls various membrane permeabilities. Injections of Ca^{2+} into nerve (Meech, 1972) or into heart (Isenberg, 1977) increase outward K^+ currents. Recently, Colquhoun et al. (1981) demonstrated that intracellular Ca^{2+} activates a nonspecific, inward-current channel in cultured cardiac cells. Besides these activation roles, $[Ca^{2+}]_i$ was also shown to control the inactivation process of Ca^{2+} current in noncardiac (Tillotson, 1979; Brehm et al., 1980; Ashcroft and Stanfield, 1981) and cardiac (Fischmeister et al.,

1981; Tsien and Marban, 1982; D. Mentrard, G. Vassort, and R. Fischmeister, manuscript submitted for publication) preparations. It is not, however, completely clear whether the observed decrease of Ca^{2+} current results primarily from a decrease in the driving force for Ca^{2+} due to an accumulation of Ca^{2+} at the inner side of the membrane (Gorman and Thomas, 1980; Brown et al., 1981, Eckert and Tillotson, 1981; D. Mentrard, G. Vassort, and R. Fischmeister, manuscript submitted for publication) or from specific channel inactivation.

We examined this question by simulating the slow inward Ca^{2+} current, I_{Ca}, in frog heart and its accompanying variations in $[Ca^{2+}]_i$. In the extreme (and unrealistic) case where all Ca^{2+} carried by I_{Ca} remains free inside the sarcoplasm, a transient accumulation, followed by a depletion of Ca^{2+} at the inner side of the membrane, was observed only when $D_{Ca} < D^0_{Ca}/100$ (Fig. 1 *a*). Although this value is half or less of the reported values of D_{Ca} in muscle (Niedergerke, 1957; Kushmerick and Podolsky, 1969; Safford and Bassingthwaighte, 1977), no significant modification in the kinetics of I_{Ca} inactivation was observed (Fig. 1 *d*). Presumably, Ca^{2+} diffuses more slowly than Na^+ or K^+ because it binds at specific binding sites. These chemical interactions would reduce the D_{app} (Eq. 16) of intracellular Ca^{2+} to a fraction of its maximal D_{Ca}. Our simulations with the second model (Fig. 2) show the occurrence of an accumulation-depletion process for a much larger value of D_{Ca} ($D_{Ca} = 0.07\ D^0_{Ca}$, Fig. 2 *c*) when the total concentration of binding sites and/or their affinity to calcium is increased. However, the overall concentration of free Ca^{2+} and, thus, $[Ca^{2+}]_i$ at the membrane is reduced, making its relatively large variations ineffective on the kinetics of I_{Ca} (Fig. 2 *d*). Under our assumptions, therefore, there cannot simultaneously be a large concentration of high-affinity binding sites for Ca^{2+} and a high free Ca^{2+} concentration near the membrane.

After deleting the inactivation parameter f and its related gating variables α_f and β_f, in Eq. 21, we tried to simulate an inactivation of I_{Ca} induced solely by a reduction in E_{Ca} due to an accumulation of Ca^{2+}. Even with a value of D_{Ca} as small as $D^0_{Ca}/10{,}000$, it required several seconds to block I_{Ca} during a voltage-clamp step to 0 mV. Another possibility is that Ca^{2+} flows across the membrane into a sequestered subsarcolemmal space (Bassingthwaighte and Reuter, 1972). With this assumption, we could simulate a waveform close to the experimental I_{Ca} observed at 0 mV voltage-clamp step, assuming that Ca^{2+} fills a space inside the sarcolemma as small as 0.8% of the cell volume. Fig. 3 shows the I_{Ca} at 0 mV as well as the I_{Ca} simulated with this assumption at various other potentials. The waveforms corresponding to potentials other than 0 mV are not supported by experimental data. If Q_{Ca} were the amount of Ca^{2+} entering the cell via the slow inward channel and needed to block I_{Ca} at 0 mV (by reducing E_{Ca} to 0 mV), assuming that there is no inactivation mechanism, Eq. 29 shows that $Q_{Ca}/2.2$ would be necessary to fully inactivate I_{Ca} at +10 mV, and $Q_{Ca}/4.84$ at +20 mV. This would lead to steeply decreasing functions of E_m both for peak I_{Ca} values and for the apparent time constant of inactivation, which are not observed in frog heart (D. Mentrard, G. Vassort, and R. Fischmeister, manuscript submitted for publication).

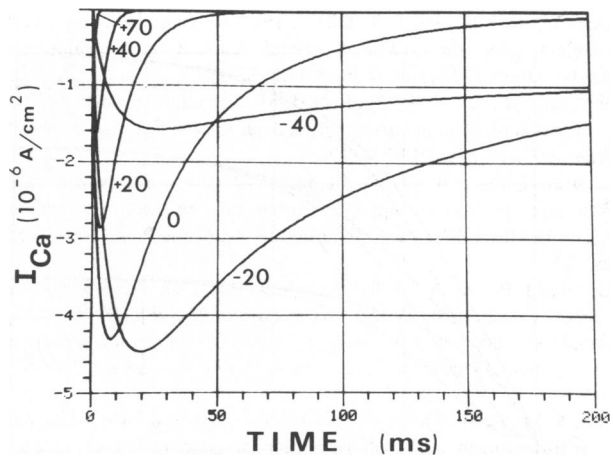

FIGURE 3 Simulations of I_{Ca} during voltage-clamp depolarizations at various potentials. No inactivation parameter was considered. The decrease of I_{Ca} is only due to a reduction in E_{Ca}, assuming that Ca^{2+} is moving through Ca^{2+} channels into a subsarcolemmal space as small as 0.8% of the cell volume.

We conclude that variations in E_{Ca} due to Ca^{2+} accumulation do not significantly affect the inactivation of I_{Ca} in frog heart. However, this may not be true in larger preparations (Levy et al., 1982). Besides, variations in E_{Ca} can also be induced by extracellular Ca^{2+} depletion (Almers et al., 1981; Fox and Krasne, 1982), although this does not occur in frog heart (D. Mentrard, G. Vassort, and R. Fischmeister, manuscript submitted for publication). Finally, the relatively large differences in our simulations between the $[Ca^{2+}]_i$ at the center of the cell and at the inner side of the membrane (Figs. 1 *a* and *b*, 2 *a*, *b*, and *c*), which result from Ca^{2+} influx, may account in part for the observed delay between the onset of electrical and mechanical activities in frog heart.

We thank Drs. R. L. DeHaan, L. J. DeFelice, and G. Vassort for helpful comments on the manuscript and we acknowledge the assistance of Mr. P. King of the Editorial Service, Dalhousie University, Faculty of Medicine, Halifax, Nova Scotia, Canada in the preparation of the manuscript.

This work was supported by grants from the Medical Research Council of Canada (MT-4128) and the Nova Scotia Heart Foundation to Dr. M. Horackova.

Received for publication 3 August 1982 and in final form 4 November 1982.

REFERENCES

Allen, D. G., and J. R. Blinks. 1978. Calcium transients in aequorin-injected frog cardiac muscle. *Nature (Lond.)*. 273:509–513.

Almers, W., R. Fink, and P. T. Palade. 1981. Calcium depletion in frog muscle tubules: the decline of calcium current under maintained depolarization. *J. Physiol. (Lond.)*. 312:177–207.

Ashcroft, F. M., and P. R. Stanfield. 1981. Calcium dependence of the inactivation of calcium currents in skeletal muscle fibres of an insect. *Science (Wash. DC)*. 213:224–226.

Bassingthwaighte, J. B., and H. Reuter. 1972. Calcium movements and excitation-contraction coupling in cardiac cells. *In* Electrical Phenomena in the Heart. W. C. De Mello, editor. Academic Press, New York. 353–395.

Blaustein, M. P., and A. L. Hodgkin. 1969. The effect of cyanide on the efflux of calcium from squid axons. *J. Physiol. (Lond.)*. 200:497–527.

Brehm, P., R. Eckert, and D. Tillotson. 1980. Calcium-mediated inactivation of calcium current in *Paramecium*. *J. Physiol. (Lond.)*. 306:193–203.

Brown, A. M., K. Morimoto, Y. Tsuda, and D. L. Wilson. 1981. Calcium current-dependent and voltage-dependent inactivation of calcium channels in *Helix aspersa*. *J. Physiol. (Lond.)*. 320:193–213.

Carslaw, H. S., and J. C. Jaeger. 1959. Conduction of Heat in Solids. Oxford University Press, London. 2nd ed. 510.

Colquhoun, D., E. Neher, H. Reuter, and C. F. Stevens. 1981. Inward current channels activated by intracellular Ca in cultured cardiac cells. *Nature (Lond.)*. 294:752–754.

Crank, J. 1975. The Mathematics of Diffusion. Oxford University Press, London. 2nd ed. 422.

Douglas, J. 1958. The application of stability analysis in the numerical solution of quasi-linear parabolic differential equations. *J. Trans. Am. Math. Soc.* 89:484–518.

Eckert, R., and D. L. Tillotson. 1981. Calcium-mediated inactivation of the calcium conductance in caesium-loaded giant neurones of *Aplysia californica*. *J. Physiol. (Lond.)*. 314:265–280.

Fabiato, A., and F. Fabiato. 1978. Calcium-induced release of calcium from the sarcoplasmic reticulum of skinned cells from adult human, dog, cat, rabbit, rat, and frog hearts and from fetal and new-born rat ventricles. *Ann. NY Acad. Sci.* 307:491–522.

Fischmeister, R., and M. Horackova. 1982. Slow inward Ca current in frog heart: theoretical evidence against a voltage-dependent inactivation. *Can. J. Physiol. Pharmacol.* 60:1185–1192.

Fischmeister, R., D. Mentrard, and G. Vassort. 1981. Slow inward current inactivation in frog heart atrium. *J. Physiol. (Lond.)*. 320:27P–28P.

Fox, A. P., and S. Krasne. 1982. Relaxation due to depletion in an egg cell calcium current. *Biophys. J.* 37:(2, Pt. 2): 20*a*. (*Abstr.*)

Gorman, A. L. F., and M. V. Thomas. 1980. Intracellular calcium accumulation during depolarization in a molluscan neurone. *J. Physiol. (Lond.)*. 308:259–285.

Hoerter, J., F. Mazet, and G. Vassort. 1981. Perinatal growth of the rabbit cardiac cell: possible implications for the mechanism of relaxation. *J. Mol. Cell Cardiol.* 13:725–740.

Horackova, M., and G. Vassort. 1976. Calcium conductance in relation to contractility in frog myocardium. *J. Physiol. (Lond.)*. 259:597–616.

Horackova, M., and G. Vassort. 1979. Slow inward current and contraction in frog atrial muscle at various extracellular concentrations of Na and Ca ions. *J. Mol. Cell Cardiol.* 11:733–753.

Hume, J. R., and W. Giles. 1981. Active and passive electrical properties of single bullfrog atrial cells. *J. Gen. Physiol.* 78:19–42.

Isenberg, G. 1977. Cardiac Purkinje fibres: $[Ca^{2+}]_i$ controls the potassium permeability via the conductance components g_{K1} and g_{K2}. *Pfluegers Arch. Eur. Physiol.* 371:77–85.

Katz, A. M. 1970. Contractile proteins of the heart. *Physiol. Rev.* 50:63–158.

Kushmerick, M. J., and R. J. Podolsky. 1969. Ionic mobility in muscle cells. *Science (Wash. DC)*. 166:1297–1298.

Levy, S., D. Tillotson, and A. L. F. Gorman. 1982. Intracellular Ca^{2+} gradient associated with Ca^{2+} channel activation measured in a nerve cell body. *Biophys. J.* 37(2, Pt. 2):182*a*. (*Abstr.*).

Meech, R. W. 1972. Intracellular calcium injection causes increased potassium conductance in *Aplysia* nerve cells. *Comp. Biochem. Physiol.* 42:493–499.

Niedergerke, R. 1957. The rate of action of calcium ions on the contraction of the heart. *J. Physiol. (Lond.)*. 138:506–515.

Page, S. G., and R. Niedergerke. 1972. Structures of physiological interest in the frog heart ventricle. *J. Cell Sci.* 11:179–203.

Palti, Y., R. Gold, and R. Stampfli. 1979. Diffusion of ions in myelinated nerve fibers. *Biophys. J.* 25:17–31.

Roughton, F. J. W. 1959. Diffusion and simultaneous chemical reaction velocity in haemoglobin solutions and red cell suspension. *Prog. Biophys. Biophys. Chem.* 9:55–104.

Safford, R. E., and J. B. Bassingthwaighte. 1977. Calcium diffusion in transient and steady states in muscle. *Biophys. J.* 20:113–136.

Tillotson, D. 1979. Inactivation of Ca conductance dependent on entry of Ca ions in molluscan neurons. *Proc. Natl. Acad. Sci. USA* 76:1497–1500.

Tsien, R. W., and E. Marban. 1982. Digitalis and slow inward current in heart muscle: evidence for regulatory effects of intracellular calcium on calcium channels. *In* Advances in Pharmacology and Therapeutics II, Vol. 3: Cardio-Renal and Cell Pharmacology. H. Yoshida, Y. Hagihara, and S. Ebashi, editors. Pergamon Press, Oxford. 217–225.

Vieth, W. R., and K. J. Sladek. 1965. A model for diffusion in a glassy polymer. *J. Colloid Sci.* 20:1014–1033.

Wang, J. H. 1953. Tracer-diffusion in liquids. IV. Self-diffusion of calcium ion and chloride ion in aqueous calcium chloride solutions. *J. Am. Chem. Soc.* 75:1769–1770.